Radiation Physics and Chemistry 188 (2021) 109621

Contents lists available at ScienceDirect

Radiation Physics and Chemistry

journal homepage: www.elsevier.com/locate/radphyschem

Cathodoluminescence, SEM and EDX analysis of CaF_2 and Tm_2O_3 pellets for radiation dosimetry applications

R. Rodríguez [a,*], V. Correcher [a], J.M. Gómez-Ros [a], J.L. Plaza [b], J. Garcia-Guinea [c]

[a] CIEMAT, Av. Complutense 40, 28040, Madrid, Spain
[b] Departamento de Física de Materiales, Universidad Autónoma de Madrid (UAM), Campus de Cantoblanco, Madrid, Spain
[c] Museo Nacional de Ciencias Naturales (CSIC), José Gutierrez Abascal 2, Madrid, 28006, Spain

ARTICLE INFO

Keywords:
Microanalysis
Cathodoluminescence
Thulium oxide
Calcium fluoride
Quenching of luminescence
Radiation dosimetry

ABSTRACT

Preparation and synthesis of luminescent materials has a special interest in medicine, industry and research due to the wide variety of applications offered by phosphors. In this study, pellets of a mixture of CaF_2 and Tm_2O_3 which were pressed and thermally treated up to 600 °C were prepared in air. Combined SEM (scanning electron microscopy), EDX (energy dispersive X-ray analysis) and CL-RGB (cathodoluminescence red-green-blue) microanalysis and, complementarily spectral CL analysis of this phosphor were performed. EDX analysis showed that the activator was homogeneously distributed in the prepared specimens. The additional CL emission can be attributed to the properties of some luminescent centers that were apparently created during the annealing. In addition, it seems that other trapping centers were created by new structural defects during the preparation process in the CaF_2 lattice. The combined techniques SEM/EDX/CL-RGB have confirmed their capabilities in the characterization of the prepared materials. This contribution provides a process and characterization methods used in the fabrication and characterization of a phosphor that can also be used to optimize the luminescent emission of other similar synthetic materials with rare earth oxides as activators.

1. Introduction

Rare-earth elements (REE)-activated materials are of great interest due to their luminescent properties. Synthesis of REE-based phosphors is usually employed in the fabrication of LEDs, lasers and luminescent detectors, with many applications in medicine, industry, and research where REE oxides are the main raw material used in the synthesis of these kinds of phosphors (Cui and Hope, 2015). In particular, trivalent rare-earth ions such as Tm^{3+} can be introduced in some matrix (e.g. CaF_2 and $CaSO_4$), enabling luminescent REE-activated materials to be fabricated (Vasconcelos et al., 2014; Madhusoodanan et al., 1999).

The creation of trapping and recombination centers and the corresponding energy levels in the bandgap provide a new electronic configuration that will be reflected in the luminescence stimulation mechanism by thermoluminescence (TL) (Madhusoodanan et al., 1999), optically stimulated luminescence (OSL) (Asfora et al., 2016), up-conversion (UC) (Cao et al., 2008) or near-ultraviolet excitation (NUV-e) (Cai et al., 2014). Electron-hole energy is transferred to the Tm^{3+} ion (Upadeo et al., 1994) when returning to the ground state and blue light is produced by the three transitions: $^1D_2 \rightarrow {}^3F_4$, $^3P_0 \rightarrow {}^3F_4$ and $^1G_4 \rightarrow {}^3H_6$. These luminescent emissions are expected when thulium oxide has been diffused in the CaF_2 matrix. However, this phosphor has previously been synthesized via wet chemical synthesis (Vasconcelos et al., 2014) and combustion synthesis (Asfora et al., 2016; Vasconcelos et al., 2016), which are protracted processes and complex infrastructures (Cao et al., 2008; Cai et al., 2014).

In this study, powders of Tm_2O_3 and CaF_2 were homogeneously mixed and pressed. This was then followed by a simple dry heating process and was preliminarily studied as a new TL material suitable for radiation dosimetry applications (Rodríguez et al., 2020). Going beyond this previous work, the structure and composition of the resulting material was characterized by scanning electron microscopy (SEM) at room temperature to identify non-uniformities or local changes in chemical composition in micrometric scale. While the EDX technique estimates the qualitative elemental composition in addition to the changes of atomic fractions in the prepared samples (Goldstein et al., 2018), the

* Corresponding author.
E-mail address: rafael.rodriguez@ciemat.es (R. Rodríguez).

https://doi.org/10.1016/j.radphyschem.2021.109621
Received 4 August 2020; Received in revised form 1 June 2021; Accepted 4 June 2021
Available online 12 June 2021

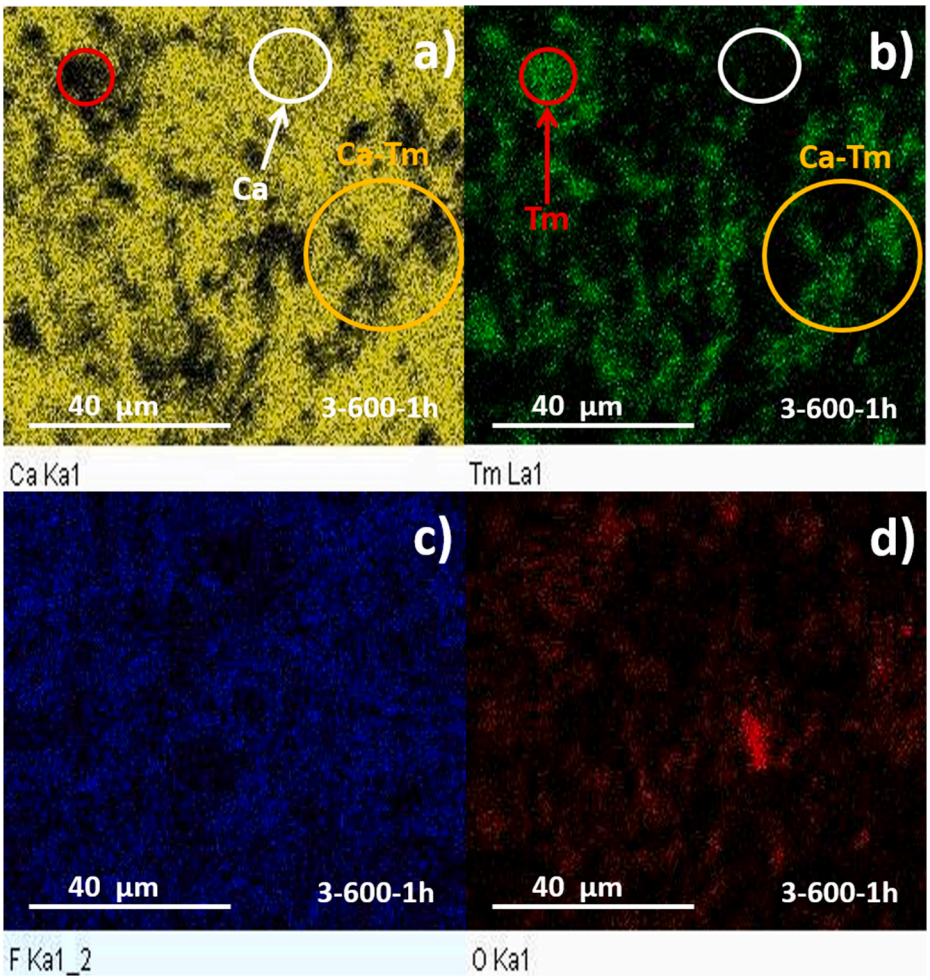

Fig. 1. ESEM/EDX maps of Ca (a), Tm (b), F (c) and O (d) in the specimen thermally treated at 600 °C for 1h (3-600-1h).

CL-RGB signal provides a filtered Red-Green-Blue (RGB) image of the luminescent center (LC) emissions with high spatial resolution (typically 1 µm) (Boggs and Krinsley, 2006). The RGB contrasted images in the visible spectrum has been compared to CL spectra for providing the luminescent characterization of the fabricated material.

2. Materials and methods

2.1. Preparation of specimens

The main feature of this preparation procedure was its simplicity. For the raw materials, Tm_2O_3 powder (99.9% of purity) was supplied by ALFA laboratory, while the CaF_2 SUPRAPUR was supplied by MERCK laboratory. The CaF_2 is a high-grade Standard Reference Material certified by the reference NIST180 Fluorspar NIST® SRM® 180, with the following metal trace basis (<150 ppm), obtained by qualitative spectrochemical analysis: Fe (0.1–1.0%); Al, Ba, Mg, Pb, Si and Sr (0.01–0.1%); Cu, K, Mn, Na, Ti and V (0.001–0.01%.); Ag and Li (less than 0.001%). The sample was milled in a manual mortar for 5 min to improve the mixing of the dopant and the CaF_2 matrix.

The sample was prepared with 3 mol% of Tm_2O_3 (to molar CaF_2) in the manner described above. The mixture of Tm_2O_3 and CaF_2 was then pressed at 60 MPa for 10 min without phase transition (Gerward et al., 1992) in a manual static powder press, which resulted in a compact sample (3-RT) around 1 mm thick. Afterwards, the compact sample was cut to obtain specimens of irregular shapes. Thereafter annealing was carried out to make pellets from these specimens, but not as a method to incorporate Tm into the crystalline fluorite lattice. Specimens were annealed for 1 h, 3 h and 7 h at 600 °C, called 3-600-1h, 3-600-3h, and 3-600-7h respectively. Annealing was done in a programmed furnace which allowed control of the heating and cooling rate of 1 °C/min in air.

This process was carried out at the *Universidad Autónoma de Madrid* (UAM) in Spain.

2.2. SEM/EDX/CL-RGB microanalysis

A Hitachi S–3000N scanning electron microscope (SEM) with a resolution of 3 nm at 25 keV was used. The EDX analyzer was an Oxford Instruments INCAx-sight model. Elemental mapping and composition spectra were obtained from the characteristic X-rays $K_{\alpha 1}$ of Ca, $L_{\alpha 1}$ of Tm, $K_{\alpha 1,\alpha 2}$ of F and $K_{\alpha 1}$ of O, employing standard references (Wollastonite, TmF_3, MgF_2, and SiO_2) with an estimated accuracy of 1%. CL-RGB emission was obtained by a Gatan CHROMA-CL2 cathodoluminescence system. The RGB filtered light emissions were recorded using a cooled array detector device (CCD) that has a detection range in the visible spectrum (400–800 nm). The red filter transmits red light in the 590–800 nm wavelength range, the green filter transmits green light in the 495–590 nm wavelength range and the blue filter transmits blue light in the 400–495 nm wavelength range. Microanalysis of the specimens was performed in the SIdI (*Servicio Interdisciplinar de Investigación*) of the UAM (*Universidad Autónoma de Madrid*) in Spain.

2.3. CL spectra

Spectral CL analysis was performed in the *Museo Nacional de Ciencias Naturales of CSIC* (Madrid, Spain). CL spectra were measured on an uncoated polished slab in low vacuum mode (40 Pa), using a Gatan

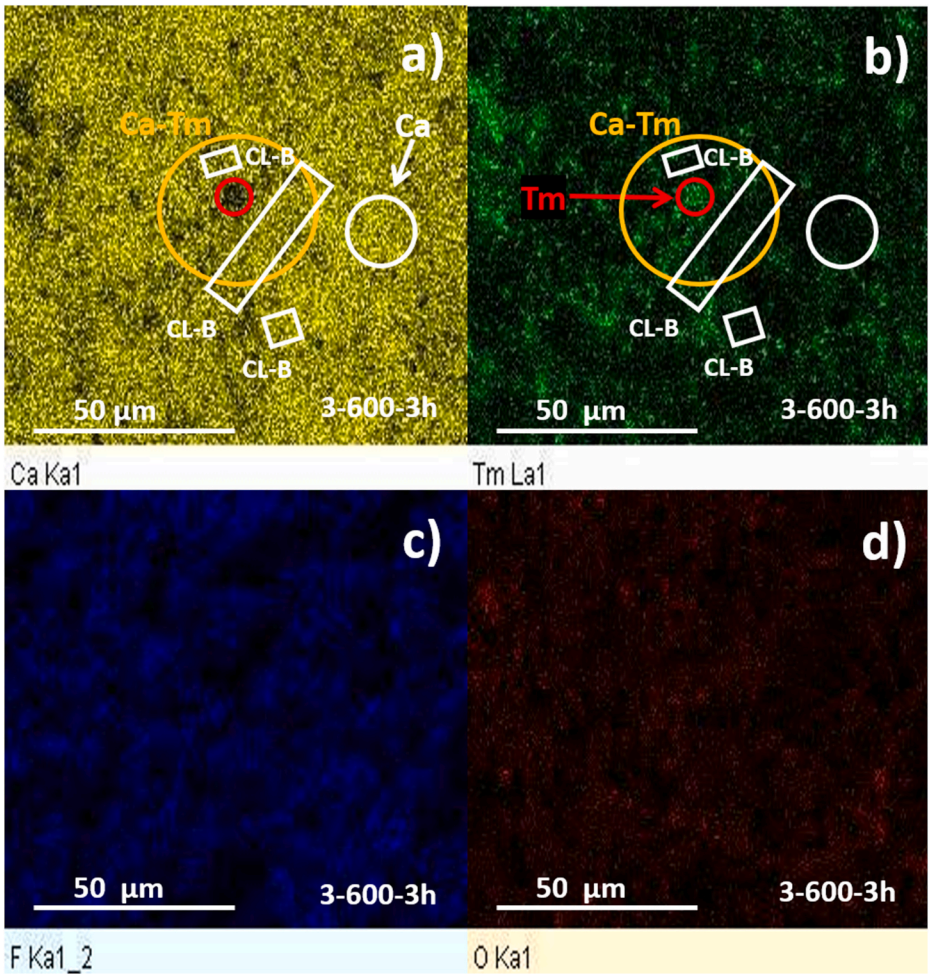

Fig. 2. ESEM/EDX maps of Ca (a), Tm (b), F (c) and O (d) in the specimen thermally treated at 600 °C for 3h (3-600-3h).

MonoCL3 detector with a diffraction grating that resolves emission spectra. A PA-3 photomultiplier tube (PMT) is attached to the SEM. The PMT covers a spectral range of 250–850 nm, and it is most sensitive in the blue part of the spectrum. A retractable parabolic mirror and the PMT are used to collect and amplify luminescence. Specimens were positioned 16.2 mm beneath the bottom of the CL mirror assembly. Excitation for CL measurements was performed with a 25 keV electron beam.

3. Results

3.1. SEM/EDX analysis

Figs. 1–3 display SEM/EDX composition maps of the thermally prepared specimens (3-600-1h, 3-600-3h, and 3-600-7h) in false colors. Maps of Ca, Tm, F and O in yellow, green, blue and red respectively, are displayed by insets (a), (b), (c) and (d). Circles indicating the presence of Ca and Tm are highlighted in the insets (a) and (b). The absence of each element is shown in black. Thus, insets (a) display the presence of Ca within white circles, while insets (b) also highlight them as a complementary absence of Tm in the area. In the same way, insets (b) display accumulation of Tm within red circles, while insets (a) also highlight them as a complementary absence of Ca in the area. Moreover, Ca and Tm mixed areas are highlighted with orange circles, where Ca and Tm co-exist. Owing to their low atomic weight, this pattern of complementarity is not followed by elements F and O, as might be expected in insets (c) and (d). In inset (b) it is seen that Fig. 2 displays smaller quantities of Tm than Figs. 1 and 3, which is evidenced by the size and number of the Tm containing areas.

Table 1 shows the results of the relative elemental composition (atomic%) that the EDX system estimated from relative weight (weight %) in the measuring areas, as well as the calculated composition of the initial mixture (blend) without treatment. The most luminescent measurement areas were chosen.

Fig. 4 displays SEM/EDX composition spectra and the mapped regions of the thermally prepared specimens, where the insets (a), (c) and (e) show that the elemental composition is practically the same within the semi-quantitative character of these EDX measurements. Estimates of EDX analysis are made with the relative values (weight%) of the signals (counts) of the chemical elements considered in the sample, which allows the atomic percentages (atomic%) to be determined directly. However, EDX does not provide the scale of those signals, as can be seen in Fig. 4, because a calibration common to chemical elements with such different atomic weights cannot be achieved. Consequently, these relative numbers are of interest as one can semi-quantitatively estimate changes in the atomic fraction of the heaviest elements (Ca and Tm), taking into account these features of the EDX technique. This is to say that on one hand the rarer elements such as Tm (2 atomic%) and O (3 atomic%) show large relative variations, mainly showed by oxygen, as expected. On the other hand, the elements with low atomic weights (F and O) also show significant differences, with respect to the true values of the mixture (blend). These limitations of EDX extend to the estimation of the atomic fraction of Ca (32 atomic%), although this has been the best estimated element due to its rather high atomic weight and its abundance in the sample. Therefore, the counts of the respective peaks are not considered precise measurement values (high uncertainties) but allow the atomic percentages to be obtained

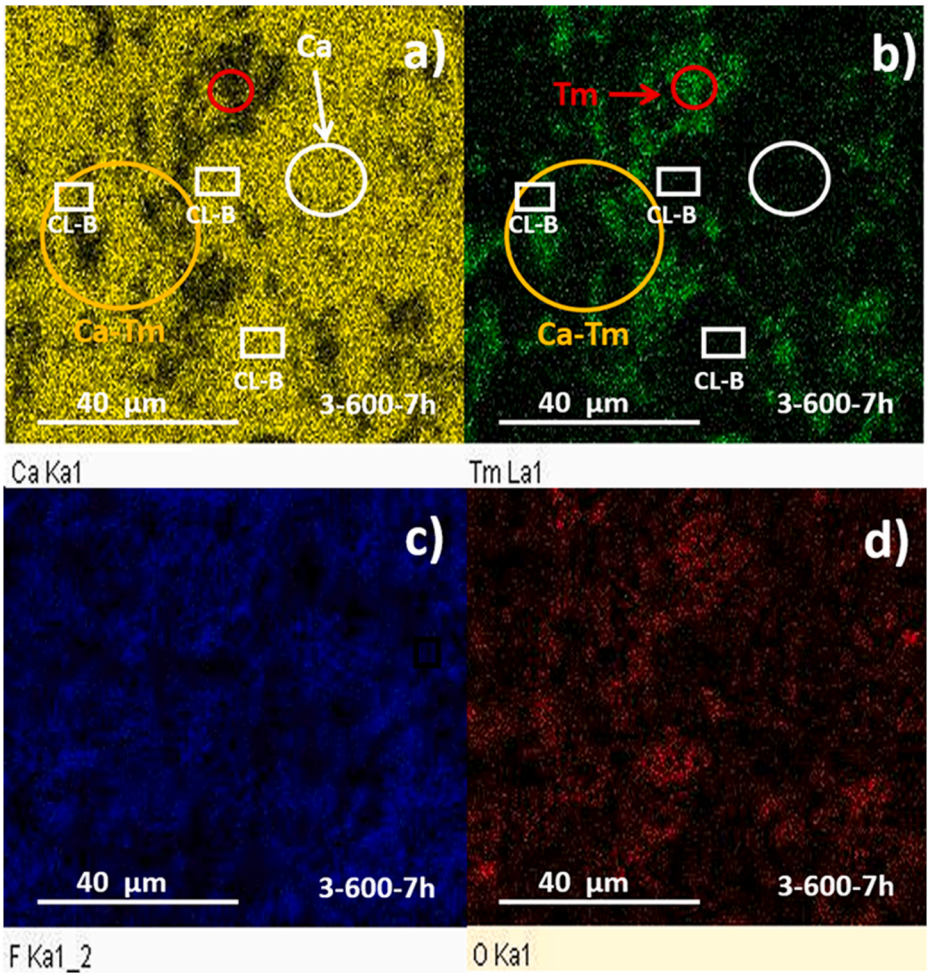

Fig. 3. ESEM/EDX maps of Ca (a), Tm (b), F (c) and O (d) in the specimen thermally treated at 600 °C for 7h (3-600-7h).

Table 1
Atomic fractions estimate (atomic%) by EDX.

Specimen	Ca	F	Tm	O
3-RT	32	58	2	7
3-600-1h	29	51	4	15
3-600-3h	30	59	3	8
3-600-7h	31	55	3	11
Blend (3 mol%)	32	63	2	3

directly. In this sense, the results show that no significant changes in composition were found due to thermal preparation of the samples.

For the SEM mapped regions, shown in the insets (b), (d) and (f), 3-600-3h sample displays a micrometric grained structure, which is in contrast to the other specimens with large accumulation areas of Tm, which are displayed as red circles. Several areas of Tm accumulation displayed a non-homogeneous distribution, although average homogeneity was maintained. Therefore, spectra and composition maps showed that the SEM mapped regions can be considered representative of each specimen regarding their average homogeneity.

Fig. 5 shows the SEM/EDX composition analysis and map of 3-RT. Note that insets (a) and (b) also display a similar pattern to that of Figs. 1–3, with the white, orange and red circles enclosing areas of Ca, Ca–Tm mixed and Tm respectively. Moreover, no significant composition changes were found among the EDX spectra of the 3-RT, shown in inset (c), and those EDX spectra of the thermally prepared specimens in Fig. 4.

3.2. SEM/CL-RGB images

CL-RGB images are displayed in insets (a, b, c, d) in Fig. 6. Violet contrasts have been recorded in the 400–495 nm wavelength range, particularly for specimens 3-RT and 3-600-1h, shown in insets (a) and (b) respectively. This displays intrinsic CaF_2 luminescence. Furthermore, a new blue emission can be seen for specimens 3-600-3h and 3-600-7h which was not found for specimen 3-600-1h. A few luminescent areas CL-B were marked with white rectangles on the CL-RGB images, as displayed in insets (c) and (d), which can be seen to show less sharpness than those of insets (a) and (b). It should be mentioned that the sharpness of the image depends on the geometry of the sample. Owing to the fact that the image is taken using a very slow shutter speed (about 1 h), samples with longer heat treatments (3 h, 7 h) seem to be more easily altered by the irradiation of energetic electrons. In spite of this, the most contrasted blue CL emission was shown by the specimen 3-600-3h.

Figs. 2 and 3 were also marked where CL emission contrasted by CL-B, as described above. It can be seen that there is almost no accumulation of Tm in these luminescent areas.

The blue emission could be contrasted because the pronounced green emission (495–590 nm) of the samples was omitted in the CL-RGB. The green emission was only analysed with the CL spectra, which is shown in Fig. 7a, b, 7c, 7d.

3.3. CL spectra

Fig. 7a presents the CL spectra of the raw materials CaF_2 and Tm_2O_3. The CL spectra of CaF_2 show two broad maxima at 290 nm and 550 nm. The first maximum corresponds to structural defects of fluorite, which

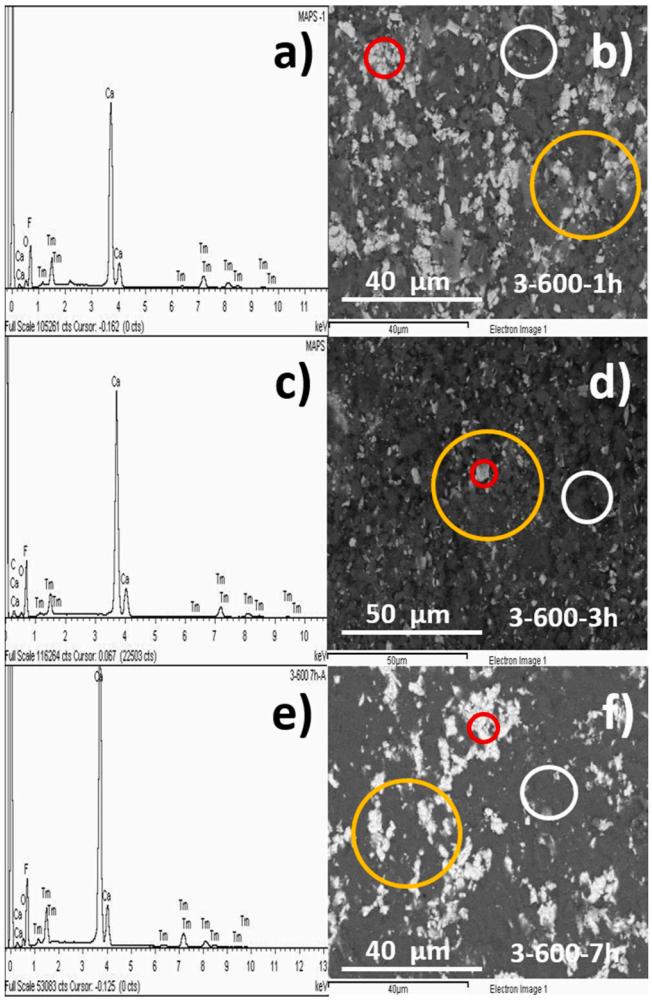

Fig. 4. ESEM/EDX of the specimens 3-600-1h, 3-600-3h and 3-600-7h: composition spectra (a, c, e) and mapped regions (b, d, f).

are described as F centre, H centre, I centre, anion vacancy and/or V_k centre (F^{2-} molecular ion), and the second to point defects of some luminescent impurity that is supposed to be Mn^{2+} at sites of Ca^{2+} because of its presence in natural fluorite (0.08%) and its strong CL emission around 560 nm (Topaksu et al., 2016), which is overlapped on the minor luminescence of the other metallic traces as shown by the wide waveband in the CL of the fluorite used. By contrast, a weak and broad CL emission from 440 nm up to 470 nm was recorded for the specimen treated at 600 °C for 3-hrs (Fig. 7c), which was not shown by the specimens treated for 1-hr and 7-hrs (Fig. 7b and d). Table 2 shows the Tm^{3+} transitions reported by spectral TL (Vasconcelos et al., 2014; Madhusoodanan et al., 1999; Wanwilairat et al., 2000), which could include the CL emissions at 454 nm and 461 nm shown by the Tm_2O_3 sample in Fig. 7a. Certainly, the identification of Tm_2O_3 emissions at 454 nm and 461 nm does not guarantee that the broad emission of the specimen 3-600-3h around 460 nm were produced by the reported transitions, although it is quite possible that thermal diffusion of Tm had occurred in the CaF_2 matrix.

CL Spectra of 3-RT and CaF_2 are similar, although reduced because the compaction with Tm_2O_3 attenuates the CaF_2 emission. Tm_2O_3 is not observed because there is little in the sample and the signal decreases due to the surrounding CaF_2.

4. Discussion

In an attempt, to find a simple annealing procedure in air, nearly pure thulium oxide and calcium fluoride were used to make pellets of a novel luminescent material. The choice of Tm_2O_3, which already has its lattice saturated with oxygen, could prevent external oxygen contamination at temperatures well below the melting point, as opposed to TmF_3 (the usual form of dopant) which oxidizes rapidly and requires an oxygen-free atmosphere. Despite the possibility of oxygen contamination with the use of the oxide form and the annealing, EDX showed no major oxygen contamination in the CaF_2 phases, although ppm (not reliably detectable by EDX) could result in luminescent changes.

The lowest accumulation of Tm in 3-600-3h suggests either the highest surface migration of Tm in the luminescent areas or simply the limited presence of the activator. Due to the fact that no composition changes were found in the analysed area, the first can be assumed.

The fundamental improvement of the CL spectra versus photoluminescence (PL) is due to the CL excitation source (25 keV electron beam) which has a much higher energy density than UV–vis light used by PL. This allows a broader typology of materials to be studied for CL characterization purposes., e.g., the high CL efficiency permits the detection and analysis of low emission samples. The photons produced by CL come from recombination either inter-band or through LCs. During the thermal preparation of pellets, many stable trapping centers can be formed like those reported for one month storage by TL of 3-600-3h in a previous work (Rodríguez et al., 2020). When inner electrons are released by energetic electron beams (25 keV), CL emission is also produced by recombination in available LCs. The contrast of CL-RGB images is due to the variation of the recombination probabilities from one area to another in the SEM mapped region. Then, the images also provide emission maps with a high resolution that displays a distribution of the LCs in the region. Specimen 3-600-7h also exhibited CL-B luminescence, shown as dotted forms, although it did not display a grained structure like 3-600-3h. The dotted luminescent sites are also related with a low concentration of Tm, as can be seen within the white rectangles. Therefore, the blue CL emission displayed by specimens 3-600-3h and 3-600-7h accords with Tm^{3+} blue emission referenced by different techniques (TL, OSL, UC, NUV-e) in Table 3. The most contrasted blue emission for 3-600-3h can be attributed to a new LC due to the highest activation in the CaF_2 matrix. This CL-B emission matches with the CL spectra found for 3-600-3h at 460 nm and, also, for Tm_2O_3 at 454 nm and 461 nm.

The most interesting result of this contribution is that the 3 h anneal produces a more uniform distribution of the cations which leads to areas of intense blue emission. Meanwhile, the 7 h anneal results in additional Tm-phase clumping and decreases the blue luminescence. This effect, known as “too long in the furnace”, resulted in two different types of luminescent structures: one intense and wide (3 h) and another weak of dotted forms (7 h), which are widespread in the CL-B analysed regions. Therefore, it may just be related to the annealing time at 600 °C. Thermodynamic equilibrium of the specimens does not last at 600 °C. Owing to the fact that the 1-hr specimen does not display any of these luminescent structures that are seen in longer annealing processes (3 h and 7 h), this balance seems to be lost beyond 1 h of annealing. Past 1 h of annealing, the CaF_2 matrix begins to exchange enough energy with the Tm_2O_3 activator to produce certain thermal diffusion effects that lead to migration of impurities and defects in the lattice. This gives rise to the greater blue emission of the sample, reaching an emission maximum before 7 h in the oven. This thermal effect is probably due to a dopant clustering effect or an enhanced oxidation process which is related to a longer annealing time. It is well known that dopant clusters, or oxygen, give rise to the quenching and reduction of dopant related luminescence (Kautsky, 1939; Omary and Patterson, 2017). CL intensity would be reduced with respect to time exposure due to non-radiative de-excitation processes that occur via energy transfer mechanisms between dopant and its environment, leading to form clusters. The resulting ground state cluster is not luminescent and, therefore, the concentration of free dopant decreases upon its clustering.

These results using different annealing times at 600 °C can be used to optimize phosphor preparation by adjusting the heating parameters for applications in radiation dosimetry (Rodríguez et al., 2020). Therefore,

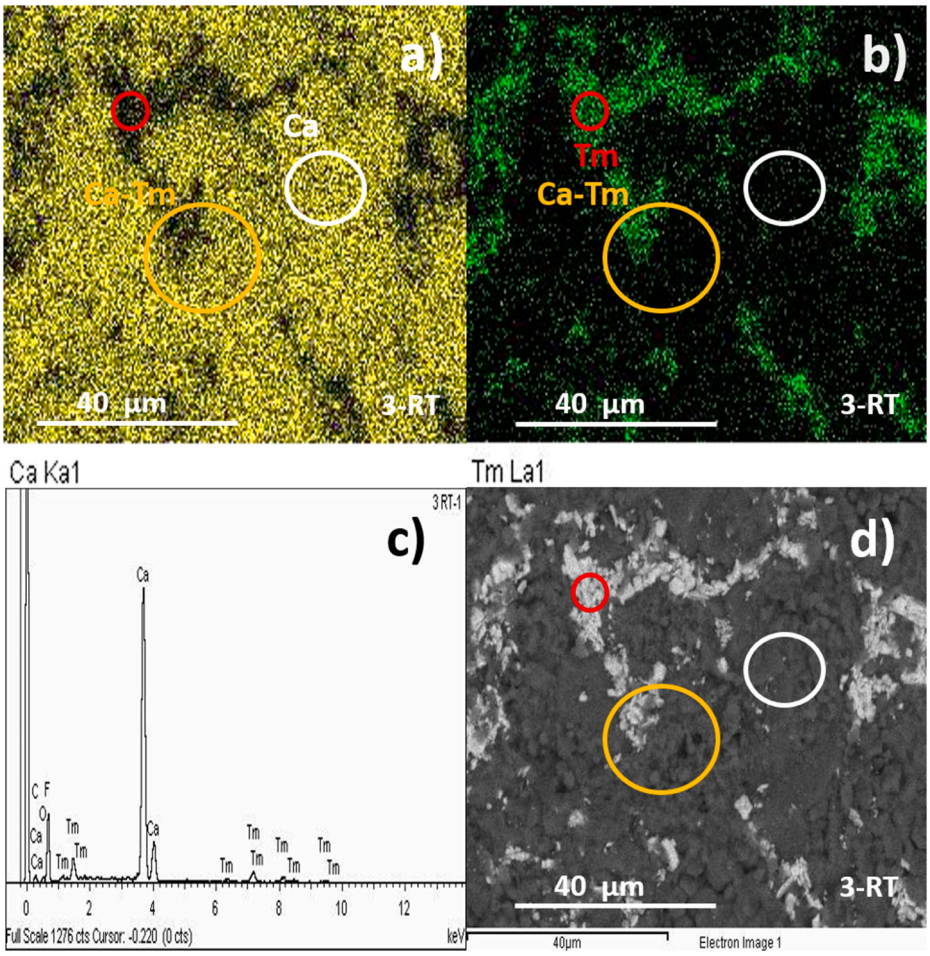

Fig. 5. ESEM/EDX of the blend specimen (3-RT): maps of Ca (a) and Tm (b), composition spectrum (c) and mapped region (d).

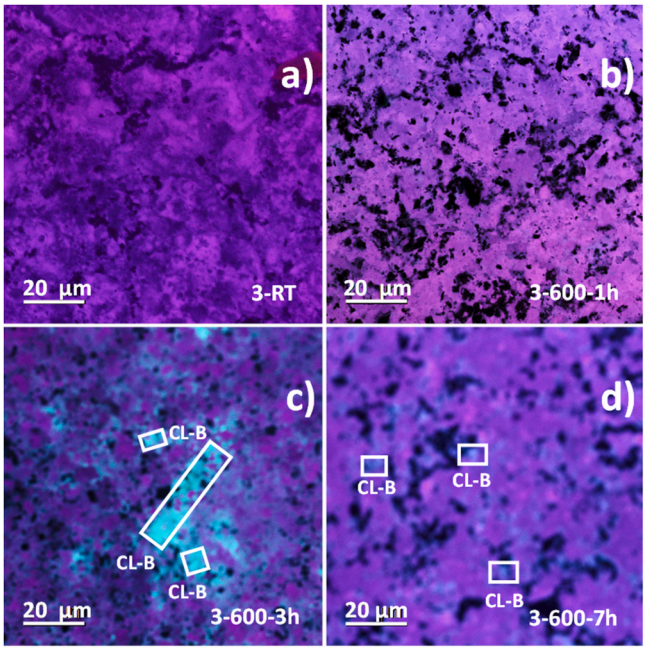

Fig. 6. ESEM/CL-RGB images of specimens: 3-RT (a), 3-600-1h (b), 3-600-3h (c) and 3-600-7h (d). ESEM/CL-RGB images were recorded at the same region of ESEM/EDX analysis.

time and temperature will operate as critical parameters to enhance luminescence in this procedure. In addition, preparation by making the finest grain and distributing it as homogeneously as possible will facilitate thermal migration for micrometric grain distribution in the matrix.

The simple preparation procedure of this low-cost material can also be used to improve thermal activation: the first one optimizing the parameters (concentration, pressure, time, temperature) of the process, and the second using other forms of the raw materials. This method can also be attempted with other materials using different REE as activators and other ionic solids with similar characteristics (lattice structure, ionic radius, electronegativity, oxidation state).

5. Conclusions

In this work, the fabrication and microanalysis characterization of an easy-to-obtain and low-cost luminescent material have presented here. A combined method of pressure (60 MPa) and thermal treatment giving rise to pellets of a phosphor consisting of a mixture of Tm_2O_3 and CaF_2 was carried out. SEM/EDX microanalysis permits to conclude that all specimens were homogeneously prepared and no elemental composition changes can be highlighted because of preparation process. On the other hand, the SEM/CL-RGB images of the phosphor displayed a LC in the blue wavelength (450–475 nm), which can be attributed to the material fabrication. The proposed optimization process and characterization methods not only allow the improvement of sensitivity of the prepared luminescent specimens, while optimizing the concentration and heating parameters, but it can also be used for the fabrication of other luminescent materials from another matrix that can be activated by REE oxides.

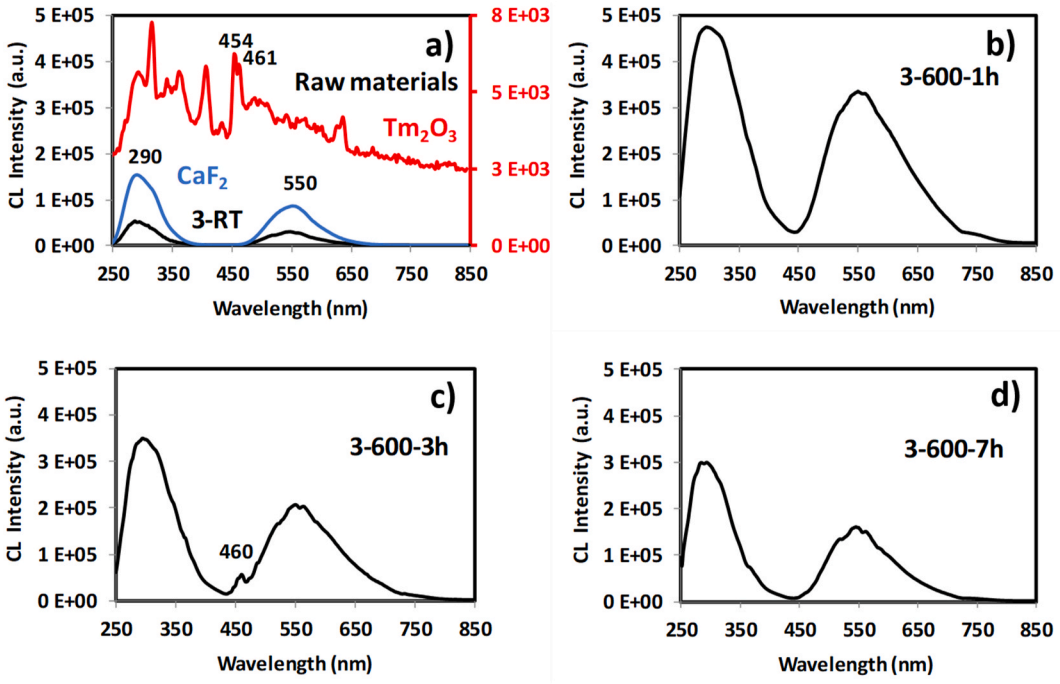

Fig. 7. CL spectra: raw materials (a) and specimens 3-600-1h (b), 3-600-3h (c) and 3-600-7h (d).

Table 2
Tm emission by spectral CL (this work) and spectral TL.

CL *(this work)* Emission (nm)	Electronic Transition (Tm^{3+})	TL Emission (nm) (Vasconcelos et al., 2014)	TL Emission (nm) (Madhusoodanan et al., 1999)	TL Emission (nm) (Wanwilairat et al., 2000)
294	$^3P_0 \rightarrow {}^3H_6$			290
316				
341		347		
361	$^1D_2 \rightarrow {}^3H_6$	361	360	356
406				
434				
454	$^1D_2 \rightarrow {}^3F_4$	452	450	
	$^3P_0 \rightarrow {}^3F_4$		455	
461	$^1G_4 \rightarrow {}^3H_6$	479	465	482
626				
636	$^1G_4 \rightarrow {}^3F_4$	652	650	650

Table 3
Blue emission of Tm by CL-RGB (this work), TL, OSL, UC and NUV-e.

CL *(this work)* Emission (RGB)	Electronic Transition (Tm^{3+})	TL Emission (nm) (Madhusoodanan et al., 1999)	OSL Emission (nm) (Asfora et al., 2016)	UC Emission (nm) (Cao et al., 2008)	NUV-e Emission (nm) (Cai et al., 2014)
Blue	$^1D_2 \rightarrow {}^3F_4$	450		457	452
	$^3P_0 \rightarrow {}^3F_4$		455		
	$^1G_4 \rightarrow {}^3H_6$	465		475	475

Author contribution statement

Rafael Rodriguez: Conceptualization, Methodology, Investigation. **Virgilio Correcher**: Resources, Supervision, Investigation. **Jose Maria Gomez-Ros**: Funding acquisition, Supervision. **Jose Luis Plaza**: Resources, Supervision.

Declaration of competing interest

The authors declare that they have no known competing financial interests or personal relationships that could have appeared to influence the work reported in this paper.

Acknowledgments

This work has been partially supported by the Spanish Ministry of Economy and Competitiveness (MINECO) under Grant FIS2015-64793-C02.

References

Asfora, V.K., Barros, V.S.M., Da Silva, R.J.G., Vasconcelos, D.A.A., Nobre, B.S., Yamato, M.E., Khoury, H.J., Oliveira, R.A., Azevedo, W.M., 2016. Optically stimulated luminescence of CaF_2:Tm. Radiat. Meas. 85, 73–77.

Boggs, S., Krinsley, D., 2006. Application of Cathodoluminescence Imaging to the Study of Sedimentary Rocks. Cambridge University Press, Cambridge. https://doi.org/10.1017/CBO9780511535475L.

Cai, L., Ying, L., Zheng, J., Fan, B., Chen, R., Chen, C., 2014. Luminescent properties of $Sr_2B_2O_5$: Tm^{3+}, Na^+ blue phosphor. Ceram. Int. 40, 6913–6918.

Cao, C., Qin, W., Zhang, J., Wang, Y., Wang, G., Wei, G., Zhu, P., Wang, L., Jin, L., 2008. Up-conversion white light of $Tm^{3+}/Er^{3+}/Yb^{3+}$ tri-doped CaF_2 phosphors. Opt Commun. 281, 1716–1719, 2008.

Cui, J., Hope, G.A., 2015. Raman and fluorescence spectroscopy of CeO_2, Er_2O_3, Nd_2O_3, Tm_2O_3, Yb_2O_3, La_2O_3, and Tb_4O_7. Journal of Spectroscopy 940172. https://doi.org/10.1155/2015/940172.

Gerward, Olsen, J.S., Steenstrup, S., Malinowski, M., Åsbrink, S., Waskowska, A., 1992. X-ray diffraction investigations of CaF2 at high pressure. J. Appl. Crystallogr. 25, 578–581.

Goldstein, J.I., Newbury, D.E., Michael, J.R., Ritchie, N.W.M., Scott, J.H.J., Joy, D.C., 2018. Scanning Electron Microscopy and X-Ray Microanalysis, fourth ed. Springer Science+Business Media LLC, New York, USA.

Kautsky, H., 1939. Quenching of luminescence by oxygen. Trans. Faraday Soc. 35.

Madhusoodanan, U., Jose, M.T., Tomita, A., Hoffmann, W., Lakshmanan, A.R., 1999. A new thermostimulated luminescence phosphor based on $CaSO_4$:Ag,Tm for application in radiation dosimetry. J. Lumin. 82, 221–232.

Omary, M.A., Patterson, H.H., 2017. Luminescence, Theory. Encyclopedia of Spectroscopy and Spectrometry, third ed., pp. 636–653

Rodríguez, R., Correcher, V., Gómez-Ros, J.M., Plaza, J.L., 2020. Preliminary study on the thermoluminescence properties of CaF_2 and Tm_2O_3 pellets. Nucl. Instrum. Methods Phys. Res. 959, 163561.

Topaksu, M., Correcher, V., Garcia-Guinea, J., 2016. Luminescence emission of natural fluorite and synthetic CaF_2:Mn (TLD-400). Radiat. Phys. Chem. 119, 151–156.

Upadeo, S.V., Gundurao, T.K., Moharil, S.V., 1994. Mechanism of thermoluminescence in CaF_2:Eu and $CaSO_4$:Eu phosphors. J. Phys. Condens. Matter 6, 44.

Vasconcelos, D.A.A., Barros, V.S.M., Khoury, H.J., Azevedo, W.M., Asfora, V.K., Guzzo, P. L., 2014. Synthesis and thermoluminescent response of CaF_2 doped with Tm^{3+}. Radiat. Meas. 71, 51–54.

Vasconcelos, D.A.A., Barros, V.S.M., Khoury, H.J., Asfora, V.K., Oliveira, R.A., 2016. Thermoluminescent dosimetric properties of CaF_2:Tm produced by combustion synthesis. Radiat. Phys. Chem. 121, 75–80.

Wanwilairat, S., Vilaithong, T., Rhodes, M., Hoffmann, W., 2000. High resolution emission spectra of CaF_2:Tm. Radiat. Protect. Dosim. 88, 307–310.